An upper ocean thermal field metrics dataset

J. E. Peak, C. R. Sampson
Naval Research Laboratory,
Monterey, CA

J. Cummings
Naval Research Laboratory,
Stennis Space Center, MS

J. A. Knaff, M. DeMaria
NOAA/NESDIS - Regional and Mesoscale Meteorology Branch,
Fort Collins, CO

W. Schubert
Department of Atmospheric Science, Colorado State University,
Fort Collins, CO

Abstract

The upper ocean provides a source of thermal energy for tropical cyclone development and maintenance through a series of complex interactions. In this work we develop a seven-year dataset of upper ocean thermal field metrics for use in tropical cyclone studies. These metrics include the surface temperature, two different measures of vertically-integrated heat content, and four different measures of vertically-averaged temperature. These upper ocean heat thermal metrics have already been used to study upper ocean energy response to tropical cyclone passage and to improve tropical cyclone intensity prediction models. The entire seven-year metrics dataset is now available on the Naval Research Laboratory web server.

1. Introduction

The ocean and the atmosphere form a complex coupled system in which heat is stored, transported and exchanged. The effect of the ocean as a source of thermal energy for the overlying atmosphere can be considerable, leading to effects such as sea breezes, tropical cyclone (TC) formation and intensification, and larger scale effects such as El Niño/La Niña Southern Oscillation (ENSO), which causes thermal variations in the upper eastern Pacific Ocean that can lead to shifts in weather patterns over large spatial scales. Quantifying heat content of the upper ocean is important in determining such air/sea interaction. The upper ocean is typically characterized by a layer that is largely homogeneous in temperature, salinity and density. This mixed layer is the source for heat and moisture fluxes to the atmosphere above, and so variations in ocean mixed layer parameters can greatly affect the overlying atmosphere. It is no surprise, therefore, that these variations in the ocean mixed layer parameters are important to atmospheric prediction and climate models.

Recent improvements in providing near real-time, three-dimensional ocean analyses (Cummings 2005) provide a data source for determining the structure of the upper ocean. The question remains how to define representative metrics to describe the thermal properties of the mixed layer appropriate for tropical cyclone intensity studies. In this paper we present several ways to define the depth of the ocean layer that interacts with the atmosphere, as well as several ways to quantify the thermal properties of the layer. The metrics employed here were suggested by Price (2009). We derive these metrics for a seven-year time period over a 65N - 65S band around the globe using the ocean analysis fields.

In Section 2 we describe data used for deriving the metrics. In Section 3 we define the metrics and present examples of the resulting 2-dimensional fields. In Section 4 we summarize the results and discuss some potential applications for the new dataset.

2. Data sets

Global ocean analyses are produced using the Navy Coupled Ocean Data Assimilation (NCODA; Cummings 2005) system. The Multi-Variate Optimal Interpolation (MVOI) scheme in NCODA uses the prior ocean analysis as a first guess. By not using a numerical model first-guess, NCODA analyses are not influenced nor contaminated by model errors, especially those associated with physical parameterization of mixing. However, the quality of the analysis is affected by a lack of data. In the case of data missing for more than 30 days profiles from the Navy ocean climatology are introduced into the analysis as synthetic observations. The purpose here is to ensure that the analysis-only system maintains a seasonal cycle.

NCODA analyses are a result of an observational data fitting approach via the NCODA MVOI on a 12-h update cycle. Conventional observational data for the analyses are obtained off the Global Telecommunications System (GTS), with satellite data obtained directly from the data provider. All data assimilated are subject to ocean data quality control procedures (Cummings, 2011). A majority of the data assimilated are available on the U.S. Global Ocean Data Assimilation Experiment (GODAE) data server (http://www.usgodae.org). NCODA assimilates satellite altimeter sea surface height (SSH) observations, satellite and in-situ sea surface temperature (SST), as well as available in-situ vertical temperature and salinity profiles from XBTs, Argo floats and moored buoys. Note that the altimeter SSH data are first converted to temperature and salinity profiles prior to assimilation (Fox et al. 2002).

Current NCODA analyses produce a twice-daily, three-dimensional analysis of temperature, salinity, geopotential and velocity on a 1/6 degree resolution grid with 34 vertical levels on stretched grid ranging from 0 m to 5000 m depth (16 levels are defined in the upper 400 m of the water column). For this study, we use archived NCODA analyses from 2005-2011 to generate a suite of two-dimensional fields of the metrics described in the following section. These derived products span the globe between 65° N and 65° S on a cylindrical grid at 0.25° resolution.

3. Derived metrics

In this section we present seven approaches to quantifying upper ocean heat content. Example grids of each metric will be presented. Graphical examples of these derived products are also produced when applicable. To facilitate comparison, data from September 15, 2010 are used in all examples presented here.

3.1 Sea Surface Temperature

The simplest metric is the Sea Surface Temperature (SST), the temperature of the top of the mixed layer. This metric has proven useful in determining conditions favorable for tropical cyclone (TC) formation and intensification. TC potential intensity is a parameter determined empirically as a function of SST (Merrill 1987, DeMaria and Kaplan 1994, Whitney and Hobgood 1997, Knaff et al. 2005; Knaff and Sampson 2009). Many empirical and theoretical models of potential intensity also have been developed (e.g., Miller 1958, Emanuel 1986, 1991; Holland 1997 and other references contained therein), which further highlight the importance of the ocean as the ultimate TC energy source. The theoretical models also include the influence of the atmosphere on the potential intensity, but under most circumstances, the ocean influence is comparable or greater than that of the atmosphere.

An example SST grid valid at Sept. 15, 2010 is presented in Fig. 1. The tropics and northern hemisphere oceans in mid-September exhibit large areas of warm SST, with some regions in the western north Atlantic, Pacific and Indian Ocean basins having temperatures exceeding 26 ° C. Many northern hemisphere tropical cyclones form and intensify in these regions.

3.2 Ocean Heat Content using 26 ° C isotherm (OHC26).

A quantification of upper oceanic heat content for TC development was first presented by Leipper and Volgenau (1972) as the integrated temperature in excess of 26° C isotherm (the commonly agreed upon lower limit for TC development) from the depth of the 26° C isotherm ($Z_{26℃}$) to the surface (0), which we will referred to as Oceanic Heat Content (OHC)[1] as defined by

$$OHC(x,y) = \rho_o C_p \int_{Z_{26℃}}^{0} [T(x,y,z) - 26]dz \quad , \qquad (1)$$

where ρ_0 = 1025 kg m^{-3} and C_p = 4025 J kg^{-1} are the mean density of and heat capacity of sea water, respectively. OHC has been used in a variety of TC research and operational applications as reviewed in Goni et al. (2009).

1. _____

[1] Leipper and Volgenau (1972) called this quantity “hurricane heat potential” . This quantity has also been referred to as “tropical cyclone heat potential” (see Goni et al. 2009, and references contained therein).

One potential disadvantage of this definition of OHC is that the 26 ° C isotherm outcrops in cooler ocean water, which leads to areas where OHC is undefined. In the Sept. 15, 2010 example (Fig. 2) this outcropping generally occurs in regions where TCs decay, but equatorward of where we prefer the metric be defined for TC studies and model development. The topology depicted in Fig. 2 shows that in some regions the warm surface conditions extend to different depths that may not be obvious from considering only the surface data.

To provide a continuous value of OHC over the entire analysis region, we use a slightly different definition of the heat content of the ocean in those regions where the isotherm outcropping occurs. We use the same vertical integral as Eq. (1), but applied over a layer defined as the level where the temperature difference from the surface is less than 1.0 ° C. Because the sea water temperatures are less than the 26 ° C reference temperature in Eq. (1), the heat content has negative values relative to sea water in regions above that temperature. In very cold water we limit the negative heat values to -240 kJ cm^{-2} for display purposes only.

Figure 3 depicts the OHC with negative values for the September 15, 2010 data. Most of the wintertime southern hemisphere oceans have negative heat content. The western parts of the north Pacific and north Atlantic have large regions of high OHC26, indicating areas where the heat content is greater due to both increased SST and deeper 26^{o} C isotherm levels. There are also significant areas where the OHC26 is between 0 and -100 kJ cm^{-2}, and these negative values could provide additional information to TC model developers.

3.3 Ocean Heat Content using 20 ° C isotherm (OHC20).

Another possible way to compute OHC is to apply the vertical integral to the 20 ° C isotherm (OHC20). This has the effect of deepening the layer over which upper ocean heat is considered to be available for interaction with the atmosphere. This could provide useful information in areas where surface stress-induced mixing might apply to deeper levels, such as under an intense atmospheric storm. The 20°C isotherm is embedded in the permanent thermocline of the tropical ocean. As such it is less likely to be influenced by local heating and cooling than integrals computed using the 26°C isotherm. The alternate definition also expands the area of inclusion before outcropping occurs (compare Fig. 4 to Fig. 2). As in OHC26, our definition of OHC20 includes negative heat values.

Figure 5 depicts the same case as in Fig. 3 except for OHC20. The high heat content areas are similar between the two approaches, but the OHC20 field shows a separate maximum in the subtropical western north Pacific.

3.4 Average Temperature to 100 m (T100).

The OHC defined in section 3.2 has several shortcomings, as pointed out by Price (2009). As originally defined, it is limited to regions where the reference isotherm does not

outcrop. In shallower waters, the ocean may not be deep enough to include the reference SST isotherm, causing a potential misrepresentation of the ocean conditions. Finally, OHC does not address static stability changes with depth in salt-stratified waters.

Price proposes that a more relevant measure of upper oceanic energy may be obtained from an average upper ocean temperature as defined by

$$\overline{T_{d\square}}(x,y) = \frac{1}{d}\int_{-d}^{0} T(x,y,z)dz, \qquad (2)$$

where the d is the depth of vertical mixing caused by a TC. Price (2009) further described two ways to define the mixing depth d in equation (2). The first assumes that the typical mixing depth associated with a mature TC passage is 100 m – a simple yet realistic assumption, and the second calculates the mixing depth directly from the ocean sounding. T100 is simple to calculate and understand, and provides a continuous measure of upper ocean heat even in relatively shallow water and outside of the tropics.

When applied to our September 15, 2010 case (Fig. 6), T100 provides a heat estimate that is representative of a layer rather than just surface SST values (compare with Fig. 1). Also in shallow water such as in the Gulf of Mexico, T100 indicates more available heat than indicated by the OHC methods (compare with Figs. 3 and 5).

3.5 Average Temperature to Temperature Difference Mixed Layer Depth (Td_ΔT_0.5)

Price (2009) suggested using d=100 m in Eqn. (2), as well as alternate definitions of d determined from the ocean sounding. The three remaining heat metrics in this study use different approaches to select the depth d. In the next three sections we select depths d to represent the level to which atmospheric interaction with the ocean water occurs.

The mixed layer is separated from the thermocline below by the barrier layer leading to stable stratification. The heat contained in the mixed layer is more available to the atmosphere than that contained in the stable layer below. Here we use the approach of Levitus (1982) which defined the mixed layer as the depth at which the temperature change from the surface temperature is 0.5 ° C.

For our Sept. 15, 2010 case, the mixed layer depth as defined by Levitus (1982) is depicted in Fig. 7. This date is at the end of the austral winter when months of cooling due to decreased solar heating and mixing from wind-driven turbulence have led to much larger mixed layer depths in the southern hemisphere midlatitudes. In the northern hemisphere (boreal summer) there is more stable stratification leading to typical mixed layer depths that are much shallower than the 100 m chosen by Price (2009).

The mean temperature of the mixed layer using a temperature difference of 0.5 ° C is depicted in Fig. 8. Comparing to T100 (Fig. 6) there are larger regions of greater Td_0.5

values over the western north Pacific and Atlantic oceans where surface temperatures are high, indicating the average is calculated over a shallower layer.

3.6 Average Temperature to Potential Density Difference Mixed Layer Depth (Td_ρθ_0.15)

Another approach to defining the mixed layer depth is to use the upper ocean potential density, the density that a parcel would acquire if brought adiabatically to the surface. For the mixed layer to be statically stable, potential density increases with depth. We define the mixed layer depth as the level where potential density increases by 0.15 kg/m^3. In the example Td_ρθ_0.15 topology (Fig. 9) and metric field (Fig. 10) it can be seen that the results are similar to those using Td_ΔT_0.5 (Figs. 7 and 8, respectively).

3.7 Average Temperature to Level of Maximum Stability (Td_MaxE)

In this metric we define the depth of the ocean barrier layer using the ocean stability (E) and the equation:

$$E = -1/\rho*(d\rho/dz) \qquad (3)$$

where ρ is the density of sea water. Stability is defined such that

$E > 0$ Stable
$E = 0$ Neutral Stability
$E < 0$ Unstable

Thus, we calculate E at each depth of the upper ocean sounding and choose the maximum stability to indicate the barrier depth. As can be seen in Fig. 11, over much of the oceans the depth of maximum stability is relatively shallow. There are some areas of deeper maximum E mainly in the north Pacific Ocean tropics. The resultant Td_MaxE metric are depicted in Fig. 12.

Discussion and conclusions

The metrics defined in the previous section have been calculated using NCODA analyses produced by the Fleet Numerical Meteorology and Oceanography Center (FNMOC). These three-dimensional high-resolution ocean analysis fields are produced twice daily. The daily 00 UTC fields are then made available on the GODAE server (http://www.usgodae.org). The data is also available via ftp at ftp://www.usgodae.org/ftp/outgoing/fnmoc/models/glb_ocn/.

The FNMOC data grid configurations have changed over the archive period as follows:

2005-06-20 to 2006-06-05: 1441 longitudes, 701 latitudes, 32 levels to 3000 m
2006-06-06 to 2006-09-22: 2161 longitudes, 1051 latitudes, 32 levels to 3000 m
2006-09-23 to 2011-12-31: 2161 longitudes, 1051 latitudes, 34 levels to 5000 m

There are a few days with some or all data missing from the archive. Table 1 lists the number of available and missing dates by year.

The metrics derived using the approaches defined in the previous section have been produced for all of the dates that have available data. The fields can be downloaded from the Naval Research Laboratory Marine Meteorology Division web site: http://www.nrlmry.navy.mil/atcf_web/nopp_ohc/. Topologies of applicable isotherm and mixed layer depths have also been derived and are available on the server. Work is underway to calculate these metrics twice daily. When operational, the results are to be posted on the GODAE server.

The derived thermal metrics have already been used in a study of the ocean response to TC passage (Knaff, et al., 2012). The results showed that passage of an average-sized, hurricane-strength TC results in typical SST cooling on the order of 0.6 ° C which persists for about 30 days. The OHC26 is decreased by about 12 kJ cm-2 and the T100 is cooled by about 0.5 ° C. These upper-ocean energy decreases were shown to persist for up to 60 days. There are ongoing efforts to update operational TC models such as the Statistical Hurricane Intensity Prediction Scheme (SHIPS, Demaria et al. 2005) and the Statistical Typhoon Intensity Prediction Scheme (STIPS, Knaff et al. 2005) using these metrics as inputs to estimate potential intensity. There are also efforts to investigate the utility of these metrics in the Logistic Growth Equation Model (LGEM, Demaria 2009).

NCODA continues to evolve and improve as well. It has been converted to a three-dimensional variational (3DVAR) analysis system (Cummings and Smedstad, 2012). The 3DVAR is operational at the Navy oceanographic production centers (FNMOC and NAVOCEANO) and is slowly replacing NCODA MVOI. More importantly, NCODA 3DVAR is in the final phase of testing as the data assimilation of the Hybrid Ocean Circulation Model (HYCOM) forecast system nearing operational status at NAVOCEANO. It is anticipated that the metrics described in paper will be generated routinely by the HYCOM global ocean forecasting system.

References:

Cummings, J.A., 2005: Operational multivariate ocean data assimilation. *Quart. J. Royal Met. Soc*., **131**, 3583-3604.

Cummings, J.A. (2011). Ocean Data Qaulity Control. In, Operational Oceanography in the 21st Century, A. Schiler, G. B. Brassington, Eds., Spring, pp. 91-121.

Cummings, J.A. and O.M. Smedstad (2012). Variational Data Assimilation for the Global Ocean. In, Data Assimilation for Atmospheric, Oceanic and Hydrology Applications - Volume 2. Xu and Park, eds (to appear).

DeMaria, M., 2009: A Simplified Dynamical System for Tropical Cyclone Intensity Prediction. *Monthly Weather Review*. **137:**1, 68–82.

____, J. Kaplan, 1994: Sea surface temperature and the maximum intensity of Atlantic tropical cyclones. *J. Climate*, **7**, 1324–1334.

____, M. Mainelli, L.K. Shay, J.A. Knaff, J. Kaplan, 2005: Further Improvement to the Statistical Hurricane Intensity Prediction Scheme (SHIPS).*Wea. Forecasting*, **20**:4, 531-543.

Emanuel, K. A., 1986: An air–sea interaction theory for tropical cyclones. Part 1: Steady-state maintenance. *J. Atmos. Sci.*, **43,** 585–604.

____, 1991: The theory of hurricanes. *Annu. Rev. Fluid Mech.*, **23,** 179–196.

Fox, D.N., W.J. Teague, C.N. Barron, M.R. Carnes, and C.M. Lee (2002): The Modular Ocean Data Assimilation System. J. Atmos. Ocean. Technol. 19:240-252.

Goni, G., M. DeMaria, J. Knaff**,** C. Sampson, I. Ginis, F. Bringas, A. Mavume, C. Lauer, I.-I. Lin, M.M. Ali, P. Sandery, S. Ramos-Buarque, K. Kang, A. Mehra, E. Chassignet, and G. Halliwell, 2009: Applications of Satellite-Derived Ocean Measurements to Tropical Cyclone Intensity Forecasting, *Oceanography*, **22**:3, 190-197.

Holland, G. J., 1997: The maximum potential intensity of tropical cyclones. *J. Atmos. Sci.*, **54**, 2519–2541.

Knaff, J.A., and C.R. Sampson, 2009: Southern Hemisphere tropical cyclone intensity forecast methods used at the Joint Typhoon Warning Center, Part II: Statistical – dynamical forecasts. *Australian Meteorological and Oceanographic Journal*, **58**:1, 9-18.

____, C.R. Sampson, M. DeMaria, 2005: An operational statisical typhoon intensity prediction scheme for the Western North Pacific.*Wea. Forecasting*, **20**, 688-699.

____, M. DeMaria, C. R. Sampson, J. E. Peak, J. Cummings, W. H. Schubert, 2012: Upper Oceanic Energy Response to Tropical Cyclone Passage. Submitted to *Journal of Climate.*

Leipper, D. and D. Volgenau, 1972: Upper ocean heat content of the Gulf of Mexico. *J. Phys. Oceanogr.*, **2**, 218-224.

Levitus, S., 1982: Climatological Atlas of the World Ocean, NOAA Professional Paper 13, U.S. Department of Commerce.

Merrill, R. T., 1987: An experiment in statistical prediction of tropical cyclone intensity change. NOAA Tech memo, NWS NHC-34, 34pp.

Miller, B. I., 1958: On the maximum intensity of hurricanes. *J. Meteor.*, **15**, 184-195.

Price, J. F., 2009: Metrics of hurricane-ocean interaction: vertically-integrated or vertically-averaged ocean temperature? *Ocean Sci*., **5**, 351-368.

Whitney, L. D., and J. S. Hobgood, 1997: The relationship between sea surface temperatures and maximum intensities of tropical cyclones in the eastern North Pacific Ocean. *J. Climate,* **10,** 2921–2930.

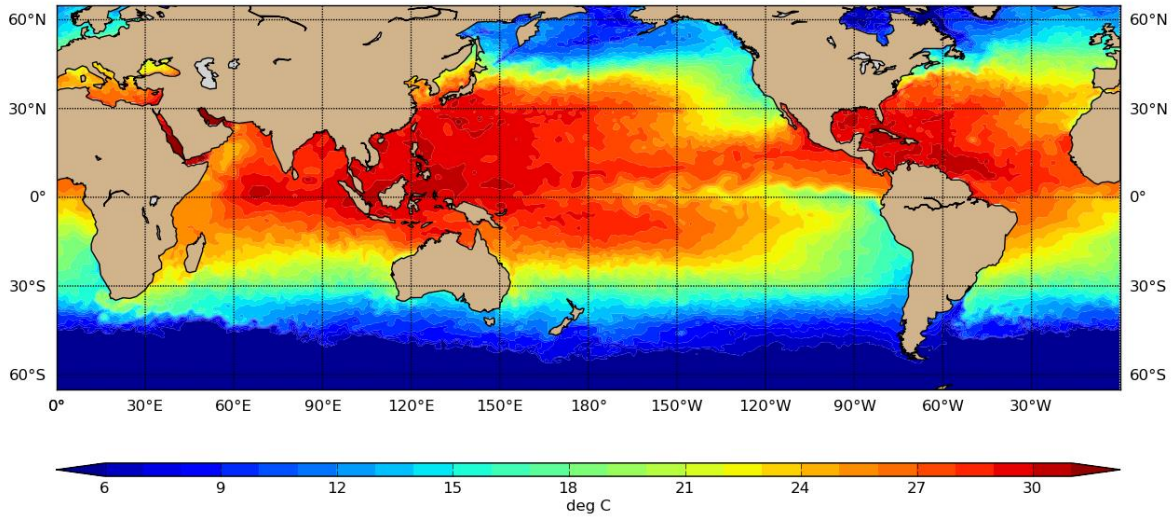

Figure 1. SST (° C) on the 0.25 ° cylindrical grid, valid 15 September 2010.

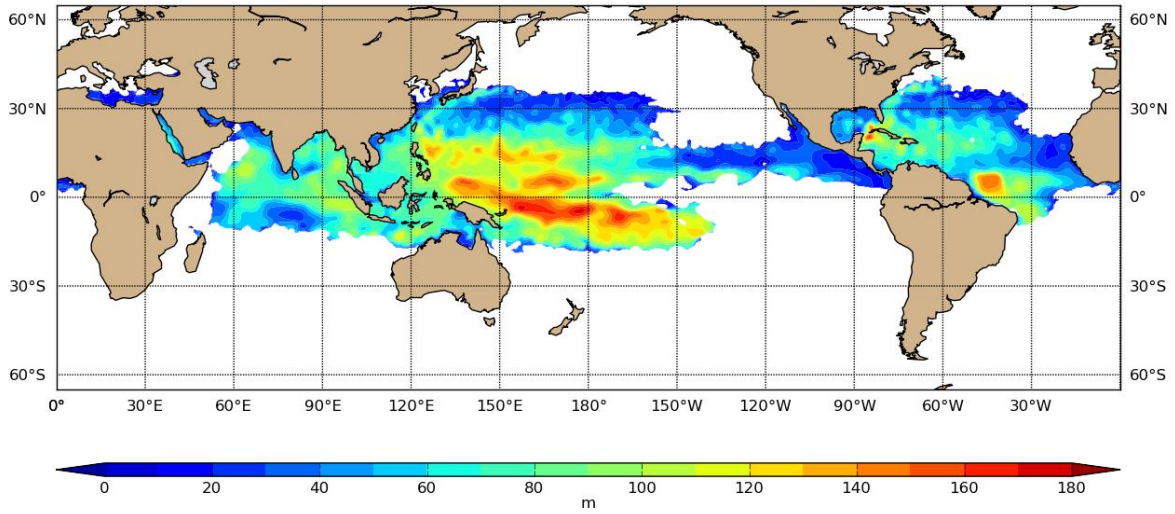

Figure 2. Depth (m) of the 26 ° C isotherm on 15 September 2010.

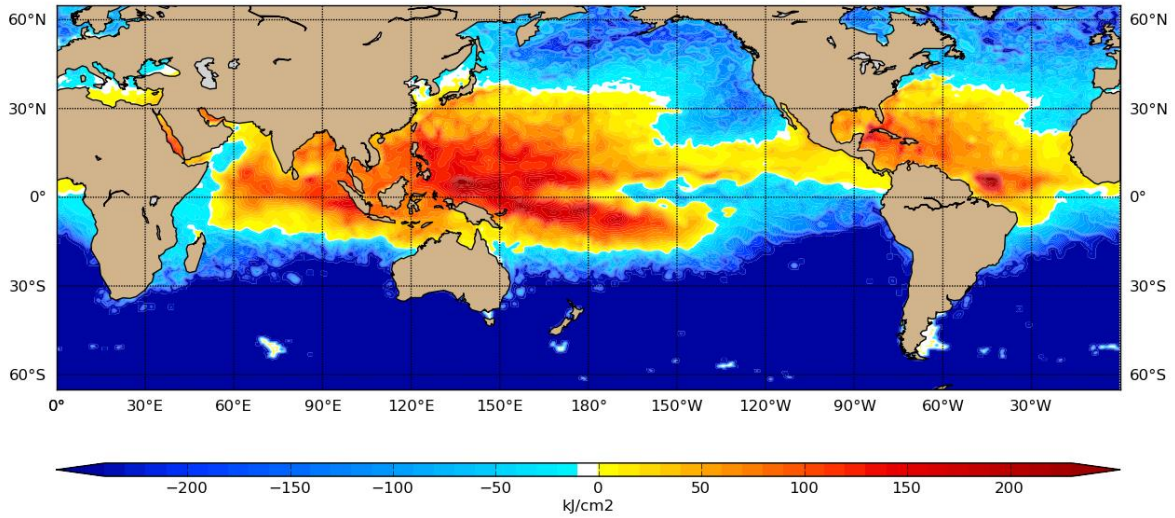

Figure 3. Ocean heat content (kg/cm^2) integrated from the surface down to the 26 ° C isotherm (OHC26) on 15 September 2010.

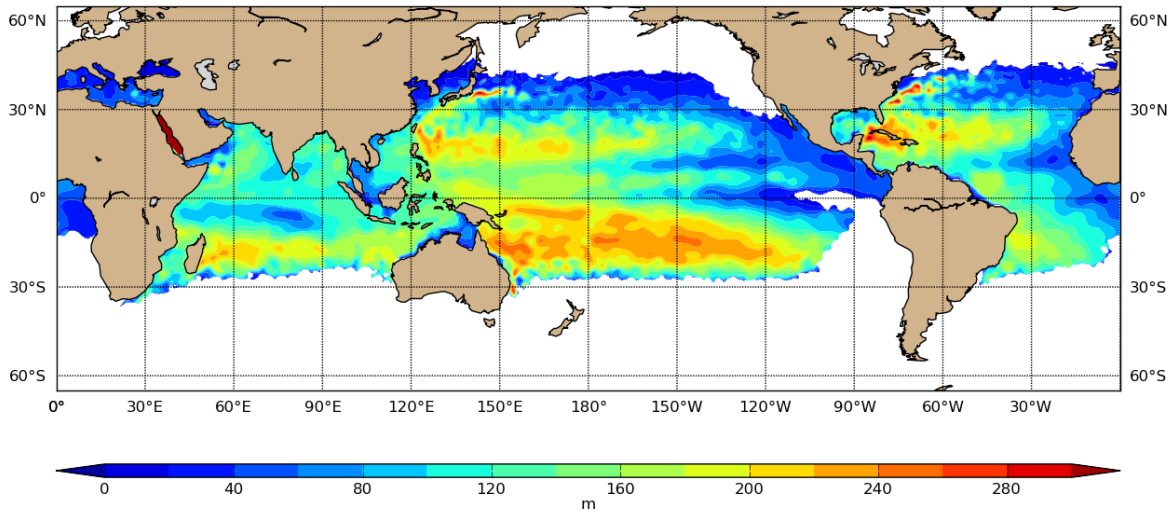

Figure 4. Depth (m) of the 20 ° C isotherm on 15 September 2010.

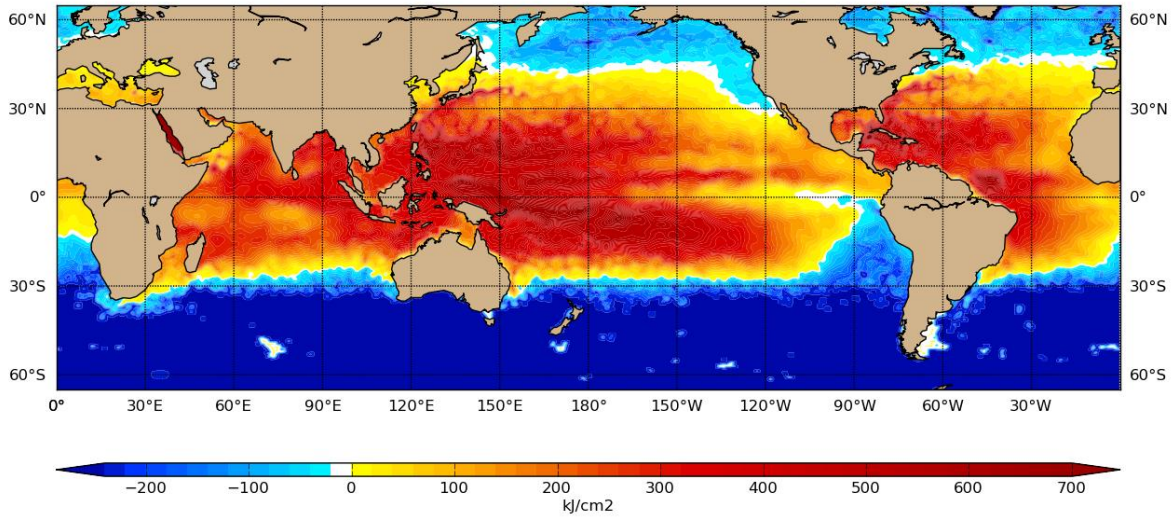

Figure 5. Ocean heat content (kg/cm^2) integrated from the surface down to the to 20 ° C isotherm (OHC20) on 15 September 2010.

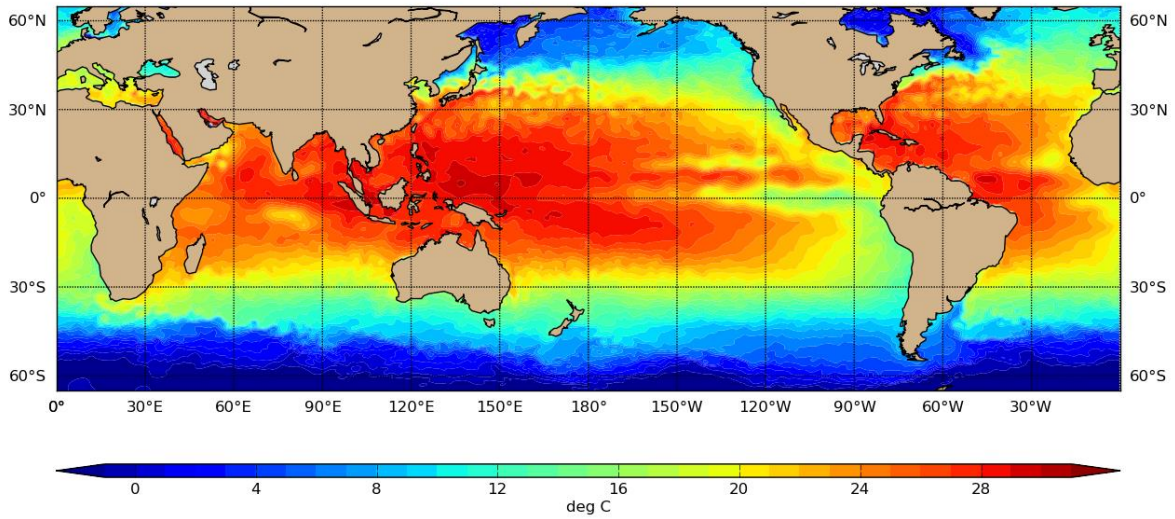

Figure 6. Layer-weighted mean temperature (° C) to a depth of 100 m (T100) on Sept. 15, 2010.

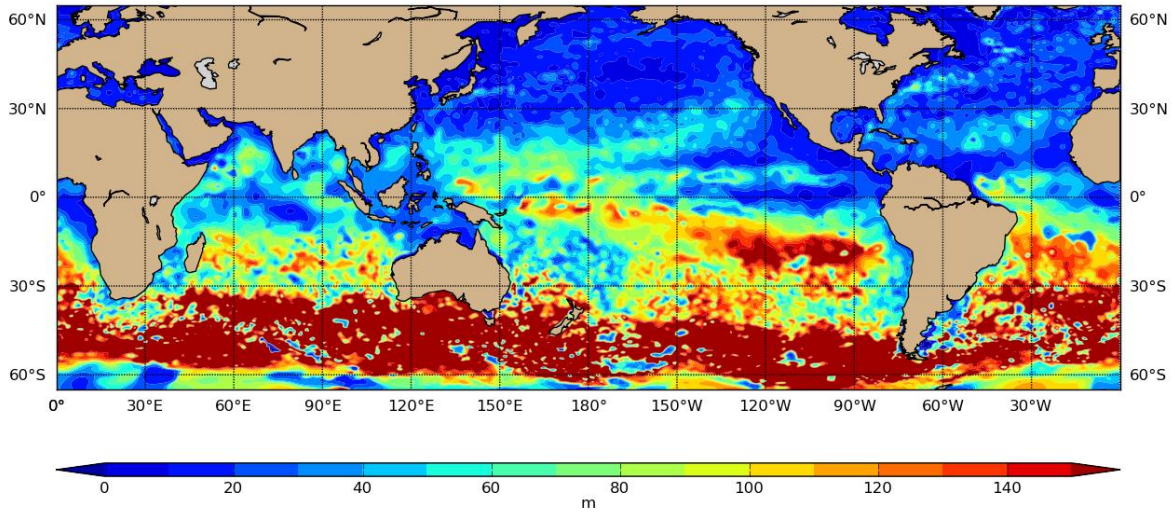

Figure 7. Mixed layer depth (m) defined by temperature difference from surface of 0.5 ° C on 15 September 2010.

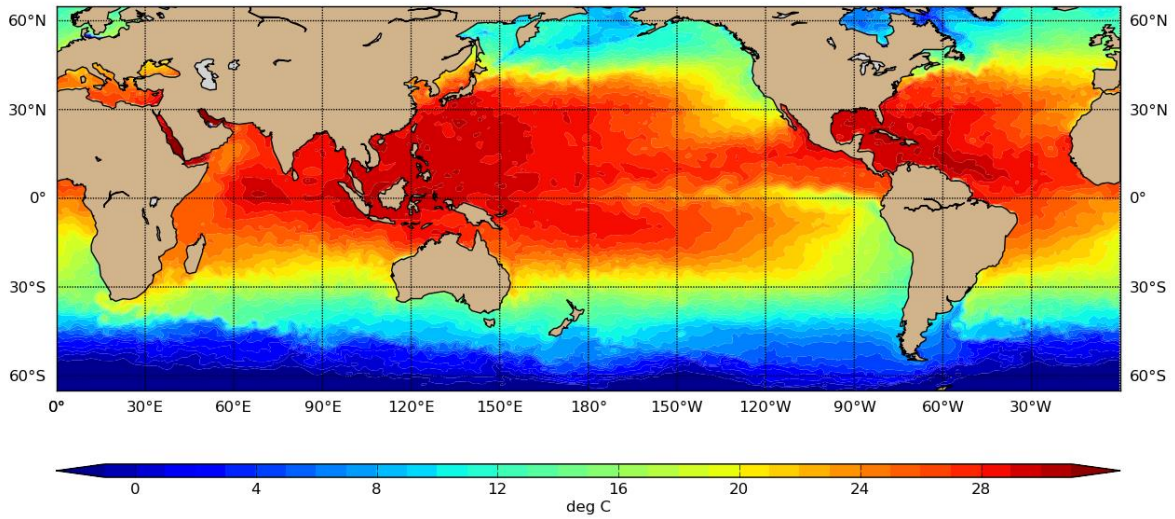

Figure 8. Layer-weighted mean temperature (° C) to mixed layer depth defined by ΔT = 0.5 ° C on 15 September 2010.

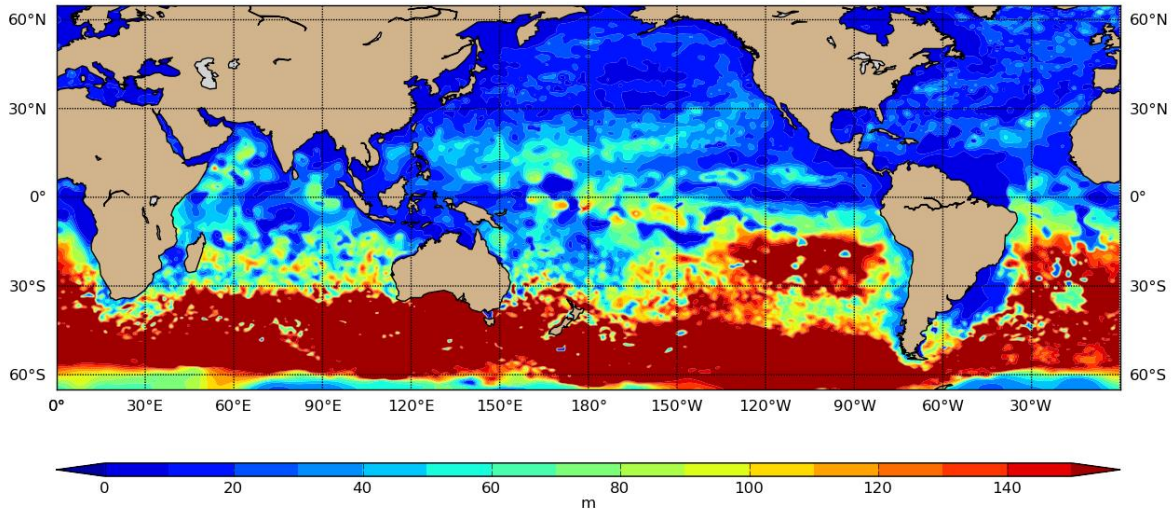

Figure 9. Mixed layer depth (m) defined by potential density difference of 0.15 kg/m^3 from surface on 15 September 2010.

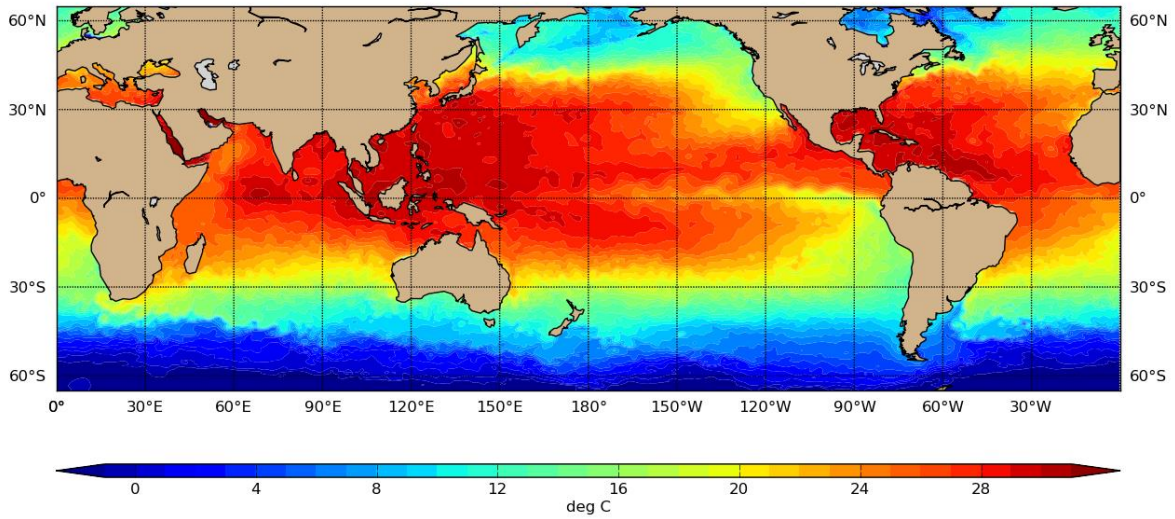

Figure 10. Layer-weighted mean temperature (° C) to mixed layer depth defined by $\Delta\rho\theta$=0.15 kg/m^3 from surface on 15 September 2010.

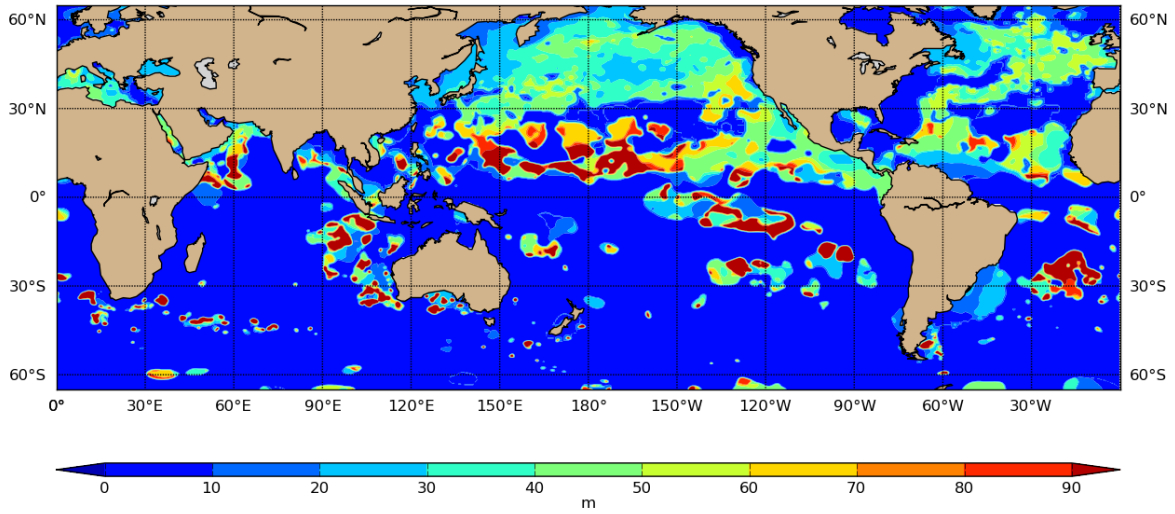

Figure 11. Depth of maximum stability (m) on 15 September 2010.

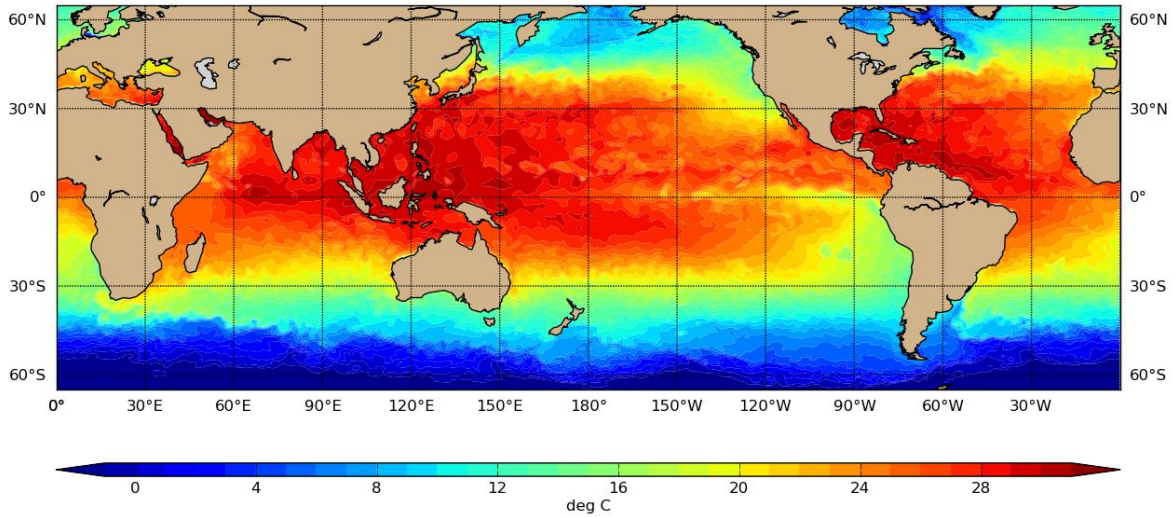

Figure 12. Layer-weighted mean temperature (° C) to the depth of maximum stability on 15 September 2010.

Table 1: FNMOC high resolution ocean analysis field availability on the GODAE server.

Year	Number of available dates	Number of missing dates	List of missing dates (month-day)
2005	192	3	08-15, 08-16, 10-28
2006	356	9	04-19, 05-31, 06-05, 06-07, 06-08, 08-23, 09-14, 09-18, 10-20
2007	363	2	05-04, 09-06
2008	360	6	05-11, 10-25, 12-06, 12-07, 12-11, 12-12
2009	351	11	02-01, 03-22, 03-26, 04-06, 04-11, 04-29, 06-04, 06-10, 08-06, 08-30, missing salinity: 03-25, 03-30, 06-15
2010	365	0	None
2011	364	1	01-26
Total	2351	32	